Design of climate station network in mountain catchments

Josef KŘEČEK[1] and Petr PUNČOCHÁŘ[2]

Abstract

In the Jizera Mountains (Czech Republic) the density of climate station network was tested in relation to spatial data interpolation, and watershed management targets. Point weather data (precipitation, air temperature, humidity and wind velocity) were interpolated by the nearest neighbourhood (NN), inverse distance weighting (IDW), spline (SPL), hypsometric (HYP) and kriging (KRI) methods. The results were assessed by the root mean square error (RMSE). The interpolation effectiveness showed the following order: HYP, IDW, KRI, NN and SPL. The advantage of the hypsometric method was recognised, particularly, by providing reasonable outputs in marginal catchments of the region and outside of the main instrumented area. However, in case of a higher density of observation points (11 hectares per station), all interpolation methods manifested comparable and realistic outputs in the focused mountain watersheds.

Keywords: mountain watershed, climate station network, precipitation, potential evapotranspiration, spatial data interpolation

Introduction

Many tasks of watershed management (water resources recharge, water quality control or flood protection) require sets of authentic climate data from point-observation networks. For many years there has been an urgent call for the improvement of climatological inputs (atmospheric precipitation, solar radiation, air temperature, humidity and wind speed) used by catchment hydrological models (BECKER, A. and SERBAN, P. 1990; COOPER, M.R. and FERNANDO, D.A.K. 2009).

WMO (1994) generally recommends the minimum aerial density of weather stations by 250 km² (eventually 25 km² on mountain islands). The

---

[1] Department of Hydrology, Czech Technical University in Prague, Thákurova 7. CZ-166 29 Prague 6, Czech Republic, e-mail: josef.krecek@fsv.cvut.cz

[2] Aon Benfield – Impact Forecasting. U Prašné brány 1, CZ-110 00 Prague 1, Czech Republic

quality of climate information in watershed scale depends on the method of aerial interpolation (and extrapolation) of the observed point data (Hay, L., Viger, R. and McCabe, G. 1998). In mountain regions, particularly, the spatial interpolation of point data is complicated by the effects of the mezo- and micro-climate. Geographic information systems are supposed to be powerful tools in the spatial application of interpolation techniques (Burroughs, P.A. and McDonnell, R.A. 1998; Hartkamp, A.D. *et al*. 1999).

The aim of this study is to compare and assess the most commonly used methods of aerial interpolation of point weather data observed in the central part of the Jizera Mountains. (Northern Bohemia, Czech Republic) (*Figure 1*).
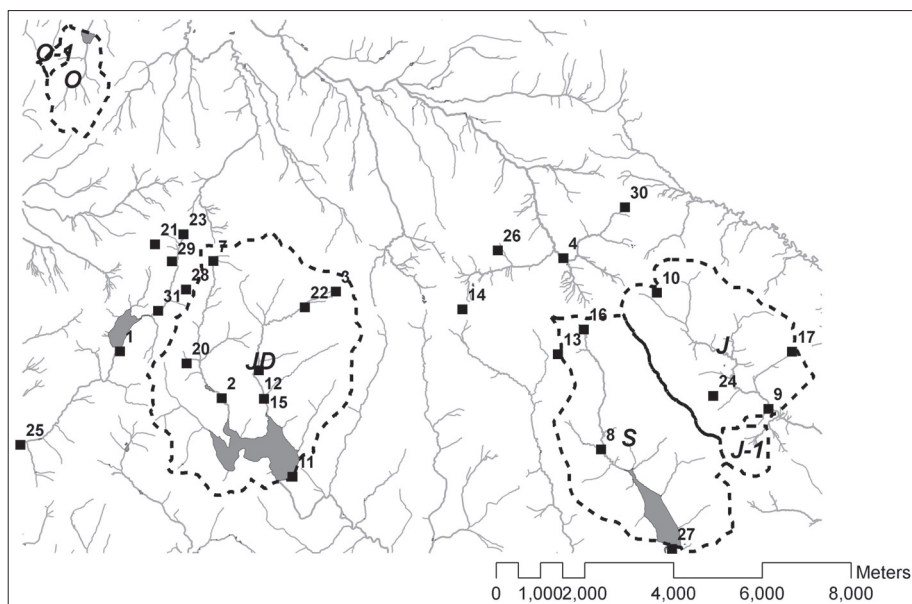

Fig. 1. Weather stations with numbers and focused basins in the Jizera Mountains. – J = Jizerka; J-1 = Jizerka-1; JD = Josefův Důl; O = Oldřichov; O-1 = Oldřichov-1; S = Sous

Material and methods

The Jizera Mountains are an important region for water resources recharge, therefore, the network of weather stations is relatively dense here. In total, 31 stations are located over an area of cca 200 km^2. The distance between the neighbouring stations varies from 0.6 to 2.8 km. All stations are instrumented by rain-gauges, 15 stations by thermometers, and 7 by anemometers.

The observation guidelines of the weather stations are provided by WMO (2009), and the spatial interpolation techniques by WMO (1994), Stein, M.L. (1999) or Sluiter, R. (2009). The following interpolation methods were used here to process the point climate data:

    1. Nearest neighbourhood method (NN),
    2. Inverse distance weighting (IDW),
    3. Polynomial functions – splines (SPL),
    4. Hypsometric method (HYP),
    5. Kriging (KRI).

The *nearest neighbourhood method* (NN) assigns the value from the nearest observation to a certain grid cell (Sluiter, R. 2009). The Thiessen concept of polygon areas corresponding to observation points was applied here. Thus, the value of a climate parameter P, representative over a catchment area A, is given by (1):

$$P = \Sigma\ (P_i A_i)/A, \tag{1}$$

where P_i = value of the parameter P, observed at the station i; A_i = area of the polygon i.

The method of inverse distance weighting (IDW) is an advanced nearest neighbour approach. The value of a certain grid cell is obtained from a linear combination of the surrounding locations. This method is based on the assumption that the weight of each observation declines with distance. The value of a climate parameter P_j in a point j is given by (2):

$$P_j = \Sigma[P_i/(D_i + S)^p]\ /\ \Sigma[1/(D_i + S)^p], \tag{2}$$

where P_i = the value of the characteristic P, observed in a point i (i = 1, 2, … n); D_i = distance of the point j from the station i; p is parameter of the weight; S = parameter of smoothness; n = number of point observations. For the aim of this study, values of S = 0, and p = 2 were applied according to Shaw, E.M. (1991).

The method of splines (SPL) is based on polynomial functions that fit trends through the observation points by x-order polynomials. To ensure that results do not show strongly oscillating patterns between the observation points, algorithms are used to smooth the resulting surfaces. Broadly speaking, polynomial functions are regarded as a good method for the interpolation of monthly and yearly climate elements but they are less suitable at higher temporal resolutions (days or hours). That approach is not recommended when the neighbouring data show significant differences (see Sluiter, R. 2009).

The hypsometric method (HYP) is a composite approach which takes account of catchment topography (Shaw, E.M. 1991). It is recommended for small or medium sized catchments in hilly regions where the relationship between climate elements and elevation is statistically significant.

The probabilistic approach of kriging (KRI) incorporates the concepts of randomness, linear regression model, geo-statistics and optimum interpolation (STEIN, M.L. 1999). That method is considered to be the best interpolation technique in case of relatively sparse point data. Kriging is also based on the recognition that the spatial variation of climate elements is often too irregular to be modelled by a simple function. Thus, the variation can be better described by a stochastic surface with an attribute known as a regionalized variable. The regionalized variable theory assumes that the value of a random variable P_j at point j is given by (3):

$$P_j = m_j + \varepsilon_j + \varepsilon'_j, \tag{3}$$

where m_j = deterministic function describing a structural component P at j; ε_j = a random spatially correlated component; ε'_j = a residual non-spatially correlated term (or noise).

When structural effects have been accounted for and the variation is homogenous, the semi-variance $\gamma\ (d)$ can be estimated by (4):

$$\gamma(d) = (1/2n) \sum (P_i - P_j)^2, \tag{4}$$

where P_i = value of climate element P, observed at the point i; P_j = value of element P at a point j (in a distance d from the point i); n = number of pairs of sample points of observations of the values of element P separated by distance d.

A plot of $\gamma\ (d)$ against d is called a semi-variogram and gives a quantitative description of the regionalised variation. An important factor of the variogram is the range which describes the distance in case of spatially independent data points. Several modifications of that approximation are mentioned by SLUITER (2009), however, in this study simple kriging applying a spherical model of the semi-variogram was used.

In this study daily precipitation amounts and daily values of mean air temperature, humidity and wind speed (data of the Czech Hydrometeorological Institute, and the Water Authority of the Elbe River collected in 1999–2007) were analysed. The raw data were filtered by the ADMS method ((SHAW, E.M. 1991) and ArcGIS/ArcInfo GIS software was applied for data processing. The success of spatial approximation was evaluated by statistical induction; the values of the root mean square error (RMSE) were calculated by (5):

$$RMSE = [(1/n) \sum (P_{mi} - P_i)^2]^{0,5}, \tag{5}$$

where P_i = parameter observed at a point i; P_{mi} = parameter modelled at a point i by the spatial interpolation from values of the parameter P in neighbouring points.

Considering the water budget in six selected watersheds (*Figure 1*), we tested the possibility to estimate realistic values of catchment precipitation (P) and evapotranspiration (ET). Potential evapotranspiration (ETP) was calculated from the daily values of climate parameters (air temperature, humidity and wind speed) by applying the FAO Penman-Monteith method (ALLEN, R.G. *et al.* 1998) corresponding to the reference crop of a height of 0.12 m, a surface resistance of 70 s/m and an albedo of 23%, adequately watered. The geomorphological characteristics of the selected basins are given in *Table 1*.

Table 1. Characteristics of the focused basins

Basin	Area (A), km²	Mean elevation (E), m	Mean slope (S), %	Length (L), km	Shape index, A/L²
J	10.41	913	9.7	4.32	0.56
J-1	1.03	927	12.0	1.14	0.79
JD	19.64	834	11.9	5.49	0.65
S	13.78	865	14.0	5.06	0.54
O	2.59	478	28.2	2.36	0.47
O-1	0.23	507	34.6	0.66	0.53

Results and discussion

Comparing the methods of interpolation, values of the root mean square error (RMSE) for modelled and observed mean annual data – precipitation (P_a), air temperature (T_a), humidity (H_a) and wind speed (W_a) – of a nine-year period (1999–2007) are presented in *Table 2*. The lower values of the root mean square error (RMSE) identify better space approximation for climate parameters.

Table 2. RMSE values for the modelled space distribution of climate parameters and methods of interpolation

Method	Precipitation (P_a) mm	Air temperature (T_a) °C	Humidity (H_a) %	Wind speed (W_a) m/s
NN	0.90	1.52	2.29	0.86
IDW	0.63	1.28	1.93	*0.52*
SPL	1.45	2.64	2.73	1.14
HYP	*0.56*	*1.13*	*1.47*	0.89
KRI	0.77	1.37	1.87	0.72

The hypsometric method (HYP) provided the best results concerning the values of precipitation, temperature and humidity; while for wind distribution, the method of inverse distance weighting (IDW) gave better outputs. That result corresponds to the significant correlation between precipitation (P_a), air temperature (T_a), humidity (H_a) and elevation (E). The estimated correlation coefficients are as follows: R = 0.757 (P_a, E), R = 0.869 (T_a, E), R = 0.728 (H_a, E), R

= 0.217 (W_a, E), by the critical value R_c = 0.254 (p = 0.01). The outputs of space interpolation (values of P_a, T_a, and H_a by hypsometric method and W_a by inverse distance weighting) for the years 1999–2007, are shown in *Figures 2, 3, 4* and *5*.

The interpolation by HYP, IDW and NN fits extreme values of the tested climate parameters by errors of ±10 %. The spline approach (SPL) tends to be a significant disfigurement of the observed extremes (up to 70%), similarly to the results of Richards, D. (1975) and Hay, L., Viger, R. and McCabe, G. (1998). Kriging (KRI) resulted in flattening the local extremes it corresponds to the findings of Stein, M.L. (1999) and Sluiter, R. (2009). The advantage of the hypsometric method (HYP) seems to be manifested mainly in a realistic extrapolation of the elevation-dependent parameters for the marginal areas of the investigated mountain region (outside of the observation network).

Concerning the interpolation of monthly data of elevation-dependent parameters, the hypsometric method was complicated by seasonal changes. Monthly precipitation showed the most significant relationship with elevation in May (R = 0.92); later it decreased to R = 0.65 (June-July), rised to R = 0.74 (September–November) and decreased to R = 0.33 (December-April).
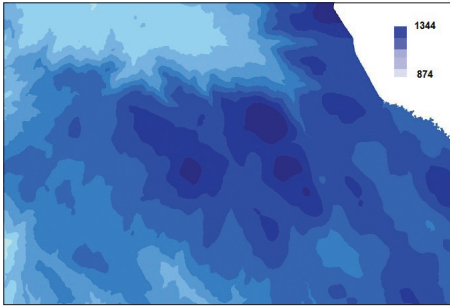

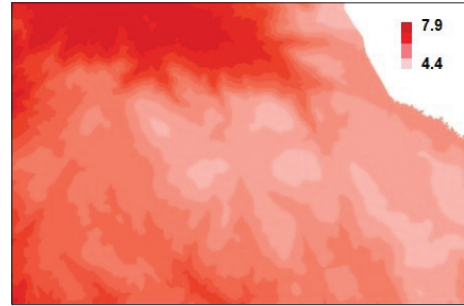*Fig. 2.* Mean annual precipitation P_a (mm) interpolated by the hypsometric method

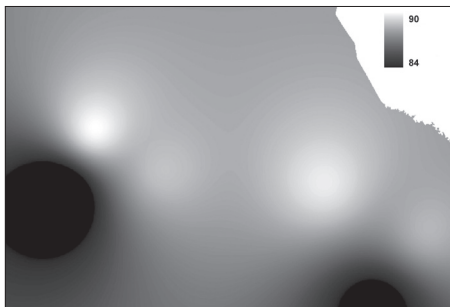*Fig. 3.* Mean annual air temperature T_a (ºC) interpolated by the hypsometric method

Fig. 4. Mean annual humidity H_a (%) interpolated by the hypsometric method
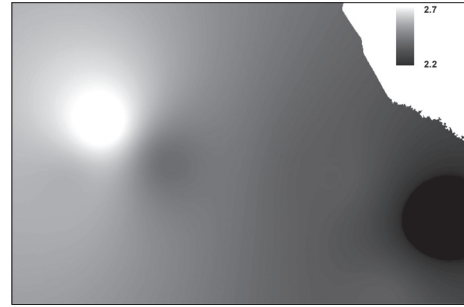

Fig. 5. Mean annual wind speed W_a (m/s) interpolated by inverse distance weighting

Potential evapotranspiration was calculated in daily steps from the interpolated daily data of temperature, humidity and wind speed. The distribution of mean annual values of potential evapotranspiration ETP_a over the Jizera Mountains region in 1999–2007 is presented in *Figure 6*.

Regarding the water budget in the six selected watersheds (*Figure 1*, *Table 1*), we suppose that aerial means of the parameters P, precipitation and potential evapotranspiration, (*P-HYP*) given by the hypsometric method are authentic. Then, differences Δ (mm) derived from the results given by alternative methods (NN, IDW, SPL, KRI) – see (6) – are shown in *Table 3*.

$$\Delta\text{-}NN = P\text{-}NN - P\text{-}HYP \qquad (6)$$
$$\Delta\text{-}IDW = P\text{-}IDW - P\text{-}HYP$$
$$\Delta\text{-}SPL = P\text{-}SPL - P\text{-}HYP(6)$$
$$\Delta\text{-}KRI = P\text{-}KRI - P\text{-}HYP$$

The percentage error ∂ (%) of aerial P-means, calculated by alternative methods (NN, IDW, SPL, KRI) versus the hypsometric method given by (7), is presented in *Table 4*.

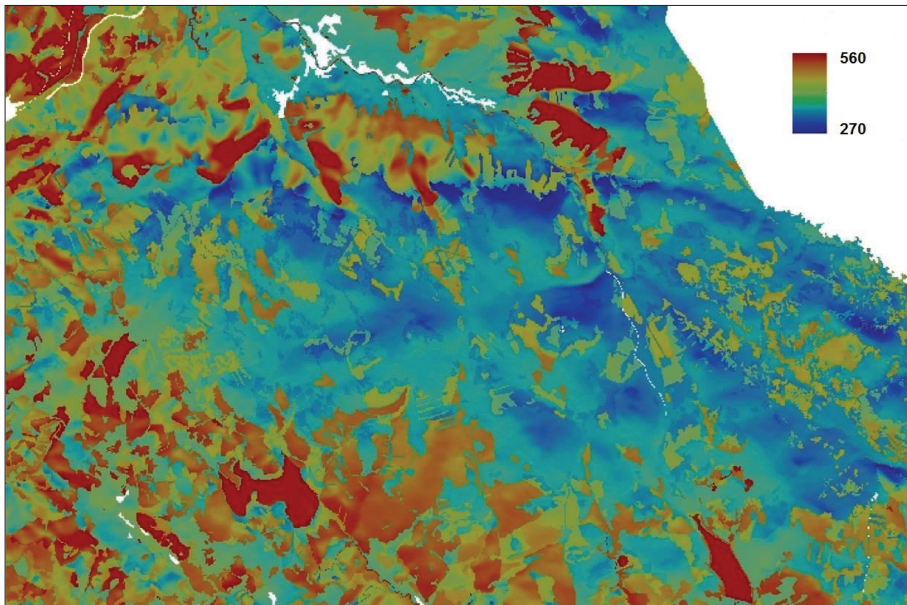$$\partial = 100\,\Delta\,/\,P\text{-}HYP \qquad (7)$$

Fig. 6. Mean annual potential evapotranspiration ETP_a (mm)

Table 3. Differences Δ (mm) between areal annual precipitation given by the hypsometric method and the methods of IDW, KRI, NN and SPL in catchments

Catchment	Number of stations	P_a-HYP	Δ-IDW	Δ-KRI	Δ-NN	Δ-SPL
		mm				
J	4	1,217	-67	-69	-82	-59
J-1	–	1,227	-99	-88	-143	-178
JD	9	1,170	-1	-1	-1	-5
S	4	1,189	-25	-25	-32	-69
O	–	973	179	217	250	394
O-1	–	955	203	235	268	330

Table 4. Percentage errors ð (%) of mean annual precipitation in the focused catchments by using interpolation methods IDW, KRI, NN and SPL

Catchment	A/N* km²	ð-IDW	ð-KRI	ð-NN	ð-SPL
		%			
J	0.25	-6	-6	-7	-5
J-1	–	-8	-7	-12	-15
JD	0.11	0	0	0	0
S	0.25	-2	-2	-3	-6
O	–	18	22	26	40
O-1	–	21	25	28	35

*A = catchment area, N = number of stations in catchments

It is evident that in catchments with a certain density of rain-gauges (11 hectares per gauge), all tested methods provide comparable and realistic outputs. On the contrary, in catchments where observations are absent, the percentage error in aerial estimates ð (%) significantly depends on interpolation techniques: ð (%) it varies from -8 to 21 (IDW), from -7 to 25 (KRI), from -12 to 28 (NN), and from -15 to 40 (SPL).

Similar errors ð (%) were found for mean annual values of potential evapotranspiration ETP_a in watersheds J (363 mm), J-1 (335 mm), JD (398 mm), S (386 mm), O (523 mm) and O-1 (514 mm) (*Table 5*). However, the accuracy of aerial evapotranspiration in catchments is limited particularly by the inadequate number of wind speed observations.

Concerning flood events, much higher errors in estimates of extreme climate events are reported by Srinivasan, G. and Sushma, N. (2005), Cooper, M.R. and Fernando, D.A.K. (2009) and Gallant, G. *et al.* (2010). Also here, for an extreme daily rainfall (observed on the 13th August 2002), rather high errors of aerial estimates were found by alternative interpolation methods: the percentage error ð (%) varies from -10 to 26 (IDW), from -13 to 26 (NN), from -16 to 34 (KRI), and from -18 to 173 (SPL) (*Tables 6* and *7*).

Table 5. Estimation errors ∂ (%) of mean annual potential evapotranspiration in the catchments calculated by interpolation methods IDW, KRI, NN and SPL

Catchment	A/N* km²	∂-IDW	∂-KRI	∂-NN	∂-SPL
				%	
J	5.20	5	8	10	7
J-1	–	7	6	9	12
JD	3.93	4	5	8	9
S	4.59	5	4	7	8
O	–	-12	-14	-21	-32
O-1	–	-10	-15	-24	-36

*A = catchment area, N = number of stations in catchments

Table 6. Differences Δ (mm) between the estimates of the areal daily rainfall (13ᵗʰ August 2002)

Catchment	Number of stations	P-HYP	Δ-IDW	Δ-KRI	Δ-NN	Δ-SPL
				mm		
J	4	207	0	0	4	16
J-1	–	209	-20	-34	-20	-28
JD	9	195	0	0	2	6
S	4	200	-10	-22	-26	-35
O	–	144	37	49	37	214
O-1	–	148	33	48	33	256

Table 7. Estimation errors ∂ (%) in aerial values of extreme daily precipitations (13ᵗʰ August 2002)

Catchment	A/N* km²	∂-IDW	∂-KRI	∂-NN	∂-SPL
				%	
J	0.25	0	0	2	8
J-1	–	-10	-16	-10	-13
JD	0.11	0	0	1	3
S	0.25	-5	-11	-13	-18
O	–	26	34	26	149
O-1	–	22	32	22	173

*A = catchment area, N = number of stations in catchments

Again, in the case of a watershed with relatively dense observation points (JD catchment) the results of all tested interpolation methods are realistic. However, with decreasing number of rain-gauges (J, S catchments with 25 hectares per gauge), the estimation error ∂ of aerial rainfall varies from -18 to 8%.

Conclusions

In the investigated mountain catchments the hypsometric method (HYP) proved to be the most effective interpolation technique for elevation-dependent climate parameters (precipitation, air temperature and humidity), see *Table 2*. The advantage of this approach is a realistic extrapolation of the data for marginal areas outside of the main observation network. For wind speed, the method of inverse distance weighting (IDW) provided the best spatial distribution because of its weak correlation with elevation. The methods of HYP, IDW and NN were able to fit extreme values of the tested climate parameters by errors of ±10% while SPL tends to be a significant disfigurement of the observed extremes (up to 70%).

For six investigated watersheds (*Figure 1*, *Table 1*), the error in estimated aerial precipitation and potential evapotranspiration depends on the density of weather stations.

With higher density of rain-gauges (11 hectares per gauge), all interpolation methods manifested comparable and realistic outputs. In catchments without observation data the output values gained by the hypsometric method were realistic and estimation errors given by alternative interpolation procedures reached almost 40% of mean annual values of precipitation and potential evapotranspiration (*Table 4.* and *5*).

In case of an extreme daily rainfall (*Table 7*) the error of aerial estimates provided by alternative interpolation techniques (NN, IDW, SPL, KRI) in marginal catchments of the studied region varies from -16 to 173%.

REFERENCES

Allen, R.G., Pereira, L.S., Raes, D. and Smith, M. 1998. *Crop evapotranspiration, guidelines for computing crop water requirements.* Irrigation and Drainage Paper 56, Rome, FAO, 300 p.

Becker, A. and Serban, P. 1990. *Hydrological models for water – resources system design and operation.* Operational Hydrology Report 34, Geneva, WMO, 80 p.

Burroughs, P.A. Mc Donnell, R.A. 1998. *Principles of Geographical Information Systems*. Oxford, Oxford University Press, 327 p.

Cooper, M.R. and Fernando, D.A.K. 2009. The effect of the rain-gauge distribution on storm water models. In *Proceedings of the 18th World IMACS / MODSIM Congress*, Cairns, Australia, 13–17 July 2009, 3500–3506.

Gallant, G., Ailie J. E., David J. and Karoly, D.J. 2010. A Combined Climate Extreme Index for the Australian Region. *Journal of Climate* 23. 6153–6165.

HAY, L., VIGER, R. and McCABE, G. 1998. Precipitation interpolation in mountainous regions using multiple linear regression. In *Hydrology, Water Resources and Ecology in Headwaters*. IAHS Publication 248, 33–38.

HARTKAMP, A.D., DE BEURS K., STEIN, A. and WHITE, J.W. 1999. *Interpolation Techniques for Climate Variables*. NRG-GIS Series 99-01, CIMMYT, Mexico, 25 p.

RICHARDS, D. 1975. *The effect of reducing rain gauge network density on goodness of conceptual models fit and predictio*n. Institute of Hydrology, Report 28, Wallingford, UK, 25 p.

SHAW, E.M. 1991. *Hydrology in Practice*. Second edition, London, Chapman & Hall, 539 p.

SLUITER, R. 2009. *Interpolation Methods for Climate Data*. KNMI Report, De Bilt, The Netherlands, 24 p.

SRINIVASAN, G. and SUSHMA N. 2005. Daily rainfall characteristics from a high density rain gauge network. *Current Science: Special Section on Mountain Weather Forecasting* 88. 942–946.

STEIN, M.L. 1999. *Statistical Interpolation of Spatial Data: Some Theory for Kriging.* Springer Series in Statistics, New York, Springer, 257 p.

WMO, 1994. *Guide to Hydrometeorological practices: Data aquisition and processing, analysis, forecasting and other applications.* Publication 168, Fifth edition, Geneva, 732 p.

WMO, 2008. *Guide to Meteorological Instruments and Methods of Observation*. Publication 8, Seventh edition, Geneva, 525 p.

NOW AVAILABLE!

Geography in Visegrad and Neighbour Countries

### Regional Socio-Economic Processes in Central and Eastern Europe – 20 Years in Transition and 2 Years in Global Economic Crisis

Edited by
Ágnes Erőss and Dávid Karácsonyi

Geographical Research Institute Hungarian Academy of Sciences
Budapest, 2011. 169 p.

During the last twenty years the erstwhile Soviet bloc countries in Central and Eastern Europe (CEE) have taken distinct routes in post-socialist development, wherein the national trends and internal regional processes proved to be in deep contrast. Responses to the challenges of the global economic crisis also varied, repeatedly brought to the surface long existing regional issues, structural problems and ethnic conflicts. Human geographers are divided in the assessment of the shifts that occurred during the past twenty years and the exchange of experience is vital for finding adequate answers to the new challenges. In order to provide a forum for discussion the Geographical Research Institute Hungarian Academy of Sciences with the generous support of the International Visegrad Fund Small Grant Programme organized a conference in order to induce the revival of contact between the institutes of geography of Visegrad Countries and their Western and Eastern neighbours. Present volume is a selection of presentations aiming to provide a deeper insight in socio-economic processes and their interpretation from geographical aspects taking place in the broader region of CEE countries.
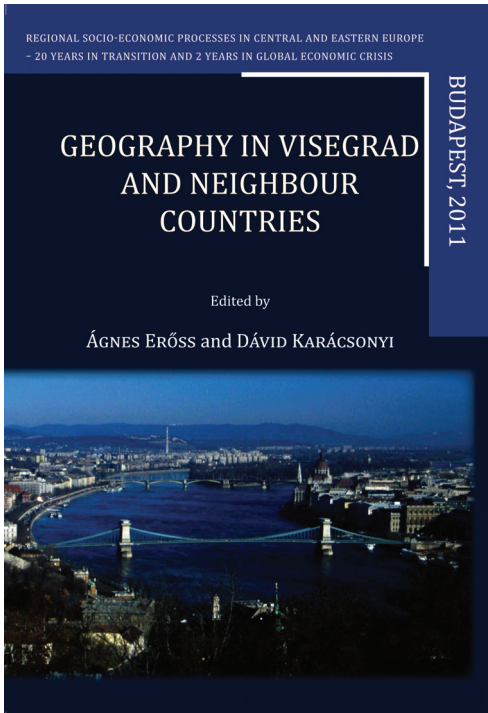
Price: EUR 10.00
Order: Geographical Institute RCAES HAS Library, H-1112 Budapest, Budaörsi út 45.
E-mail: magyar@sparc.core.hu